

GRAD Method and Code for Nonstationary Continuum Mechanics Problems

A.A. Bragin, V.A. Suchkov, A.S. Shnitko

Russian Federal Nuclear Center – Zababakhin Institute of Technical Physics (RFNC-VNIITF)
Snezhinsk, Chelyabinsk region

Introduction

The presentation with the same title took place at the Third Joint conference on Computational Mathematics in Los Alamos in 1995. It was made by Victor Suchkov who is the founder and chief scientist of GRAD method [1]. The general principles of the method and organization of GRAD code complex were presented. The model verification was given on the examples proving the technique and code correctness by means of the comparison of simulation results and the exact solution. The subject of the present talk is the technique validation. First of all I will recall the general principles of the complex organization, and then describe briefly physical and mathematical models. Afterwards I will present the simulation results in comparison with the experimental data.

Basis of GRAD technique

GRAD method and code solve nonstationary inhomogeneous continuum mechanics problems by means of computer. Hydrodynamic and elastic-plastic models are used to describe material flow. Smearred shocks and detonation waves are simulated. The necessary set of equations of state is included. Different kinetics models are developed to simulate detonation-induced transformation of explosives into explosion products. These include a kinetic model for high explosives, and semiempirical and semiconductor detonation models for low explosives. In modeling elastic-plastic flows, it is possible to consider material cracking (from one crack to two to three to break) with a failure criterion based on maximum principal stresses. The method of concentrations is used to treat large deformations.

GRAD method is inhomogeneous; it can be adapted to solving a problem. System calculated is partitioned into suite of domains on some criterion. Each domain has its own difference mesh. Basic variables are laid out on mesh cells and vertices. So we deal with topological and physical net domain structure (problem section), for which difference continuum mechanics equation related to the accepted model are solved.

Problem calculation is carried out through the domains each with the inherent time step. In different domains different models may be used: hydrodynamics, elastic-plastics, and the one-rate model of multiple material flow. Communication between the domains is implemented via boundary conditions so that parallel computation through the domains is possible on multiple-processor. For computation we use mainly Lagrangian co-ordinates; domains interface admit slip-boundary conditions. In general, the contact borders are described by two suites of points from the adjacent domains. In order to achieve conformance between the points of such borders, special algorithms for determining the neighborhood of the points are applied. Reconciliation between the points of the contact borders is attained by the boundary conditions providing the continuity of the velocity and surface forces normal components.

To maintain quality of the mesh in the domains, there exists a possibility of arbitrary movement of the mesh nodes. If the movement is non-Lagrangian then the flows of homogeneous and multiple materials through the border are calculated subject to the possible location of material interfaces. Intense mesh distortion in the domain or its fragment can be handled by the local recalculation of the mesh and variables, when keeping the number of points constant. During the calculation initially chosen problem section can conflict with the nature of material flow having varied, for example if fresh contact breaks occur or some domains degenerate. In this case the regular computation is interrupted and new problem section is created: the new system of domains is chosen, new appropriate meshes are initialized, recalculation of the variables from the old section to the new is carried out (global recalculation), etc. The new problem section may as well embody the domains of the old one. After defining a section suitable for the new state of flow, regular computation is recommenced. The procedure

of creating a new problem section, considering the choice of new domains system, depends substantially on specific problem and can hardly be formalized. Here one should use prior information obtained for the specific classes of problems. The regular computation of complicated problems may be interrupted several times to create a new section. The more ordinary problems can be calculated up to the end without interruptions.

GRAD complex contains codes for calculation one-, two- and three-dimensional non-stationary flows. Two-dimensional technique Grad-2 is the basis of the GRAD method, which is designed for calculating plane and axial-symmetric flows using second-order accurate finite difference scheme “cross” in Lagrangian coordinates. In the advection phase first-order accurate schemes are used for calculating mass, momentum and energy flows. The GRAD-1 difference scheme is obtained from the GRAD-2 difference scheme using the condition of flow symmetry (plane, cylindrical, spherical). GRAD-2 technique is taken as a basis for three-dimensional GRAD-3 technique with third spatial Euler variable added. We use modified GRAD-2 method for plane sections in Euler direction: the third component of velocity is calculated and also gradients and Euler variable flows are taken into account. Here Euler flows are calculated on the hybrid first- or second-order accurate switch scheme. GRAD-3 code complex is organized so that main variables arrays and boundary arrays are treated as two-dimensional sections in the third (Euler) spatial direction. Step calculation is implemented by split method: one half step for calculating two-dimensional section by GRAD-2-like step calculation code, another half step for calculation in Euler direction. All service resources of GRAD-2 complex are included into GRAD-3.

Physical and mathematical models

Under ISTC Project №2040 the work on creating code complex for simulating ceramic specimen pressing has been carried out. Paper /2/ presents detailed overview of the existing theoretical and semi-empirical models of rigid bodies behavior under dynamic load. The equation system describing elastic-plastic continuum medium flow consists of differential conservation laws and the following constitutive relations: an equation of state, stress tensor deviator flow law, failure model; porous medium behavior model.

Conservation laws

In the Cartesian rectangular coordinates X_i ($i = 1,2,3$), treating $X_1 = x$, $X_2 = y$, $X_3 = z$ we have

$$\begin{aligned} \rho \dot{u}_i &= \sigma_{i,j}, \\ \rho \dot{V} &= u_{i,j}, \\ \rho \dot{E} &= \frac{1}{2} \sigma_{i,j} (u_{i,j} + u_{j,i}) + \text{div}(\kappa \cdot \text{grad} T) \end{aligned} \quad (1.1)$$

These equations are sequent from momentum, mass and energy conservation relations correspondingly. We use ρ for density, $V = 1/\rho$ is specific volume, u_i – mass velocity array, $\sigma_{ij} = -P\delta_{ij} + S_{ij}$ stress tensor, S_{ij} – its deviator, P – stress, δ_{ij} – Kroneker symbol, E – specific internal energy, T – temperature, κ – coefficient of thermal conductivity, $f_{i,j} = \frac{\partial f_i}{\partial x_j}$. The point above function means full (substantial) time derivative. Equal indices i,j assume summation.

Stress tensor deviator flow laws

Constitutive relations for the stress tensor deviator S_{ij} designate models for elastic-plastic deformation. In isotropic body approximation they can be written in the form of Prandtl-Rase’s relations

$$\dot{S}_{ij} = 2\mu\dot{e}_{ij} - \lambda S_{ij}, \quad (1.2)$$

where $\lambda \geq 0$ is a scalar dissipative function with rotary component missing, μ is the elastic shear modulus, \dot{e}_{ij} – strain rate tensor deviator. The construction of the function λ designates the flow model. In particular, the model of the ideal elastic-plastic Meases' body with yield strength Y depending only on thermo-dynamical state corresponds with the function

$$\lambda = \begin{cases} \frac{3\mu}{Y^2} S_{ij} \dot{e}_{ij} - \frac{\dot{Y}}{Y}, & S_{ij} S_{ij} = \frac{2}{3} Y^2, \\ 0, & S_{ij} S_{ij} < \frac{2}{3} Y^2. \end{cases} \quad (1.3)$$

The shear modulus dependence on the density, temperature and equation of state relation is assumed as

$$\mu = \frac{3}{2} \frac{1 - 2\nu_0}{1 + \nu_0} \cdot \eta_T \cdot \rho \cdot \left. \frac{dp}{d\rho} \right|_{S=\text{const}} \quad (1.4),$$

where S – entropy, ν_0 – Poisson coefficient under normal conditions, η_T – temperature multiplier. Quasi-static yield strength Y_A is simulated by the dependence on plastic strain ε , pressure and temperature:

$$Y_A = [Y_0 + f(P)] \cdot \eta_\varepsilon(\varepsilon) \cdot \eta_T(T) \quad (1.5)$$

In (1.5) η_ε is a multiplier responsible for strain hardening (or weakening). In case of the strain-hardening material we assume $\eta_\varepsilon(\varepsilon)$ to be the same as in SG model:

$$\eta_\varepsilon = \min \left\{ \eta_\varepsilon^{\max}, \left(1 + \frac{\varepsilon}{\varepsilon_*} \right)^a \right\}, \quad (1.6)$$

regarding ε_* , a и η_ε^{\max} as constants. The function $f(P)$ is defined for positive pressures; it is assumed to be continuously increasing, up to value $Y_{00} - Y_0$, and to have continuous linearly pressure dependent first derivative:

$$Y_0 + f(P) = \min \left\{ Y_{00}, Y_0 + \alpha P \left[1 - \frac{\alpha P}{4(Y_{00} - Y_0)} \right] \right\}, \quad (1.7)$$

where α and $Y_{00} > Y_0$ – material constants, $\alpha P \leq 2(Y_{00} - Y_0)$.

When calculating in Cartesian coordinates by concentration method, one-rate model is used. In mixed cells stress tensor and specific internal energy are calculated using the condition of proportional volume increments. The average pressure in mixed cell (or the medium pressure) is obtained from volume concentrations:

$$p = \sum_i \beta_i p_i,$$

where p_i – the pressure of i component, $\beta_i = V_i/V$ – the volume concentration of i component.

Parameters for determination of environment stress tensor such as Poisson coefficient, yield strength and strengthening constants, are calculated similarly. The medium specific internal energy is obtained from mass concentrations:

$$E = \sum_i \alpha_i E_i,$$

where E_i – the specific internal energy of i component, $\alpha_i = M_i/M$ – the mass concentration of i component.

Models of detonation

In GRAD complex different expressions for explosives decomposition rate are implemented for simulating detonation waves. I will point out some of them.

1. Model kinetics of transformation of explosives into explosion products for high explosives.

$$\frac{\partial g}{\partial t} = C_g W(1 - g)$$

Here g – mass concentration of the explosion product, $W = W(\rho)$.

2. Semi-empirical model of detonation macrokinetics for low explosives, suggested by Rykovanov, G.N., Eskov, N.S. et al /3/

3. Semiconductor model of TATB detonation initiation, suggested by Grebenkin, K.F. /4/.

$$\frac{d\xi}{dt} = \exp\{F[T(t)]\} \quad \text{npu } t - t_f > t_1(T_f)$$

$$F(T) = \begin{cases} F_1 + A_1 \cdot [T(t) - T_1] & \text{npu } T(t) \geq T_1 \\ F_1 - A_2 \cdot [T_1 - T(t)] & \text{npu } T(t) < T_1 \end{cases}$$

$$t_1(T_f) = K \cdot \exp\{F[T_f]\} \quad T(t) = T_f + A \cdot (P(t) - P_f) + B \cdot (P(t) - P_f)^2$$

In contrast to semi-empirical models, the last one emanates from the specific micro-physical model of heterogeneous explosive decomposition and is based on the results of computer simulating burn wave propagation from the hot spots. The parameters of implemented macrokinetics have certain physical meaning. Their values can be defined without using experimental data on detonation initiation. Moreover, this model describes the effect of strong dependence of TATB shock wave sensitivity on temperature.

Validation of GRAD technique

Simulation of stress profile in the 2.1GPa amplitude wave

This problem is one-dimensional, plane. Spatial mesh step is equal to 0.1 mm. Mie-Gruneisen equation of state relation is used with Gruneisen coefficient $\Gamma = 2$, $c_0 = 5.33$ km/s, $n = 3$, $\rho_0 = 2.705$ g/cm³. Simulation results are compared with the experimental data [5].

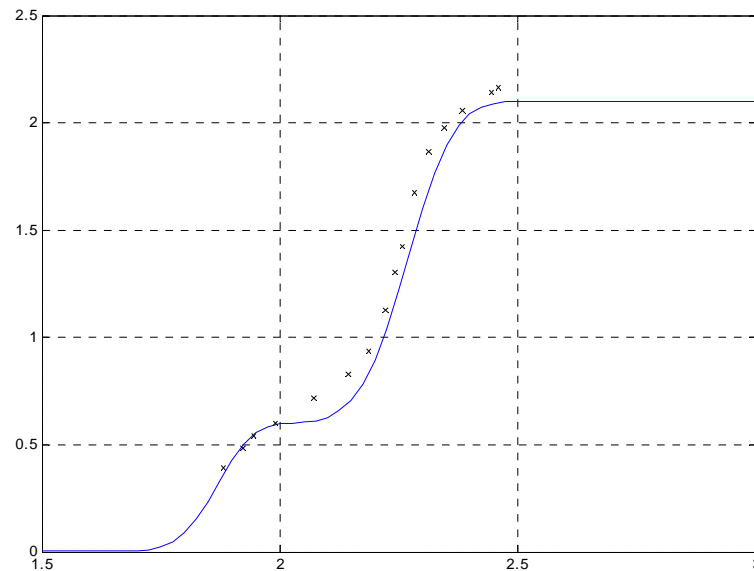


Figure 1. Stress dependence on time. Firm line is for numerical data, markers – for experiment. Wave amplitude 2.1 GPa, specimen thickness 12.5 mm.

Simulation of impact of cylinders on rigid wall

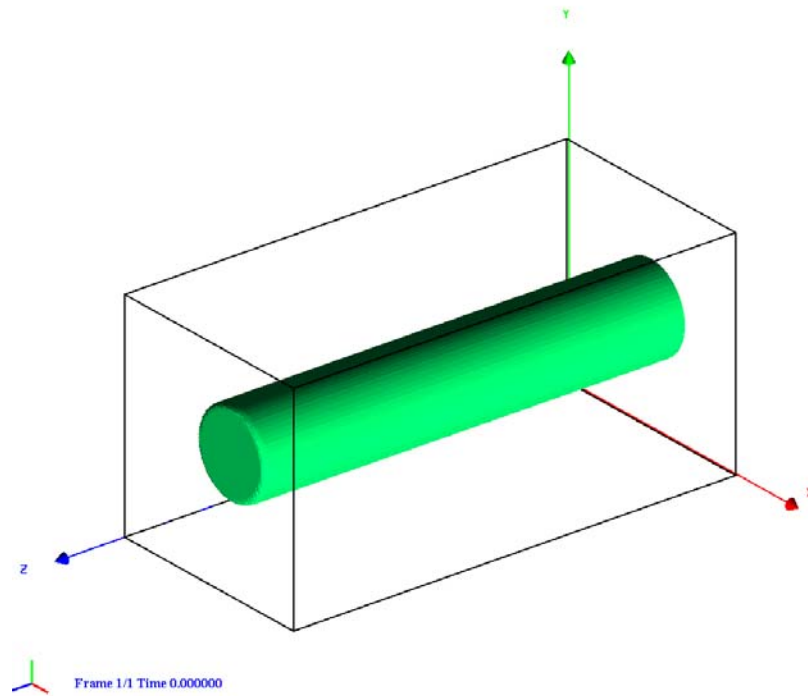


Figure 2.

The impact of aluminum cylinder on the rigid wall has been simulated. The cylinder diameter is 0.64 cm; its height – 3.177 cm; initial velocity – 0.2 km/s. Calculations are carried out in Cartesian coordinates for elastic-plastic multiple material. Figure 1 shows the initial system state in the form of equiscalar surface for aluminum volume concentration equal to 0.5. The equation of state parameters for aluminum are the following: $\rho_K=2.708 \text{ g/cm}^3$, $\gamma=3.0$, $n=3.0$, $\nu=0.34$, $Y_0=0.29$, $y_1=1.1$, $\sigma_{\text{Mex}}=2.0$. The second material in domain is air. All boundaries have zero normal velocity.

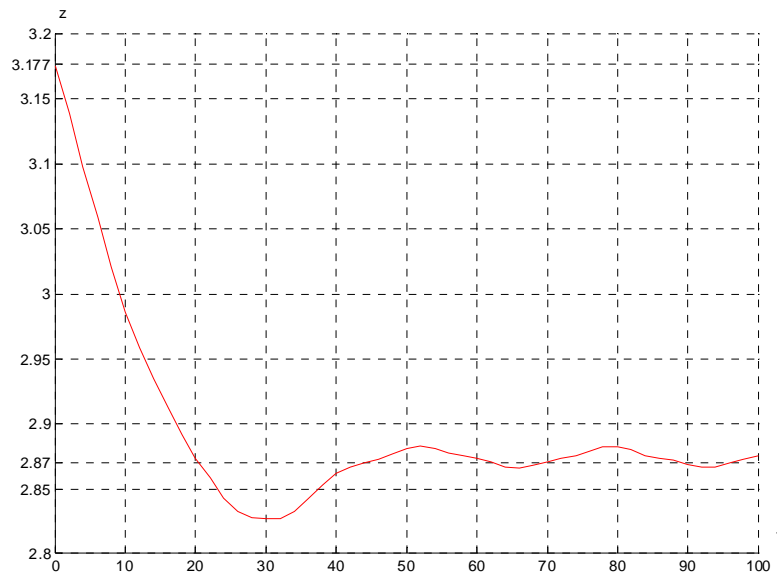


Figure 3. Rod length dependence on time. Rod free end position is determined by the position of equiscalar surface with bulk concentration 0.5.

The similar calculations have been carried out for uranium, steel and copper rods. The experimental data are taken from /6/.

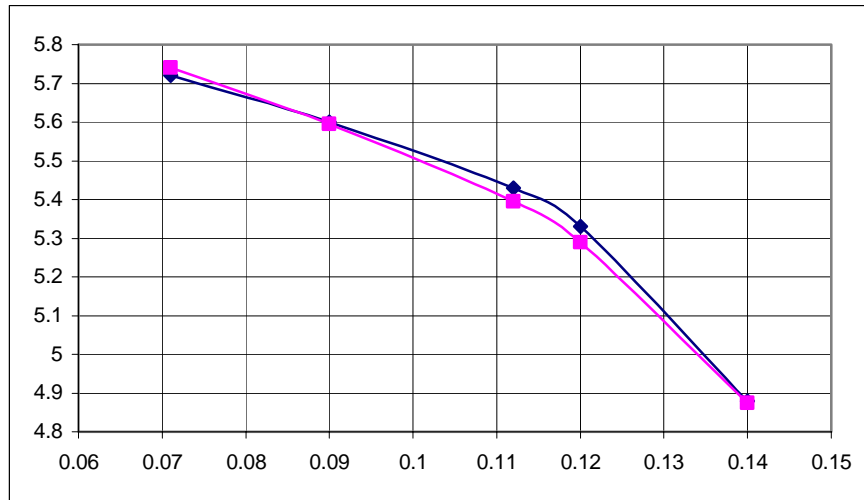


Figure 4. The uranium cylinder final length [cm] dependence on impact velocity [km/s]. Black line is for the experiment, raspberry – for GRAD calculation.

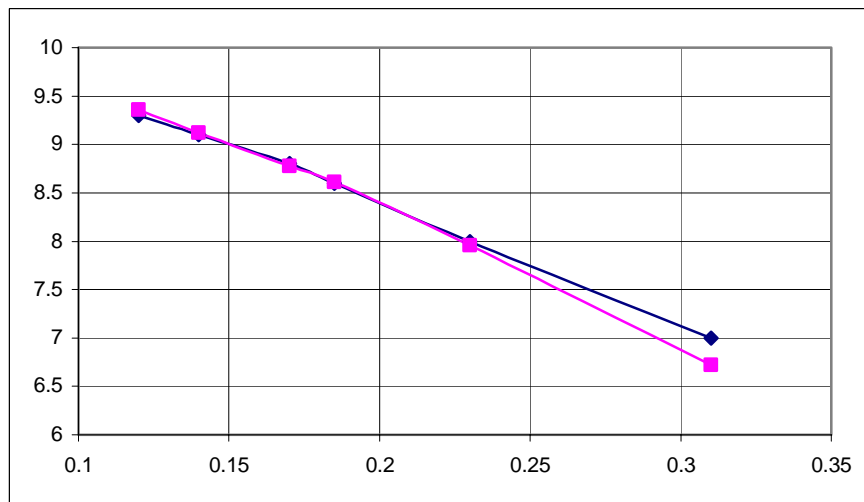


Figure 5. The steel cylinder final length dependence on impact velocity. Black line is for the experiment, raspberry – calculation with $Y_0=0.45\text{GPa}$, $\alpha=1$, $Y_{\max}=1.5\text{GPa}$.

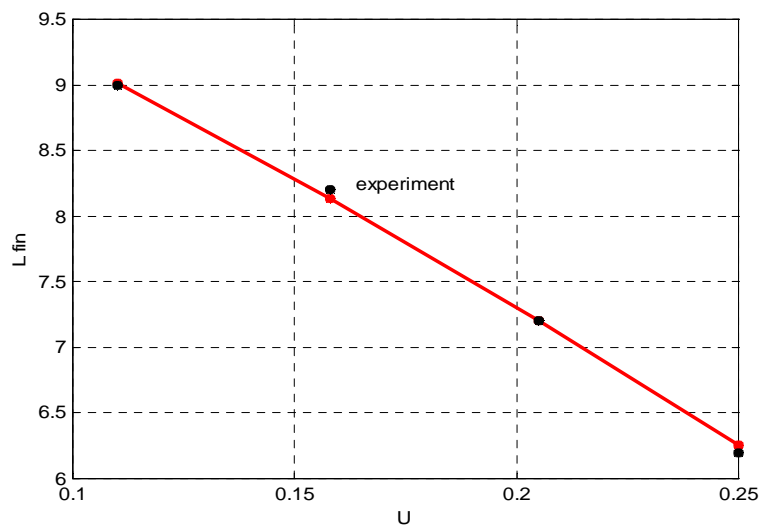


Figure 6. The copper cylinder final length dependence on impact velocity. Black line is for the experiment, raspberry – calculation with $Y_0=0.36\text{GPa}$, $\alpha=1$, $Y_{\max}=0.4\text{GPa}$.

Simulation of profile specimen pressing

The following pictures show the initial geometry.

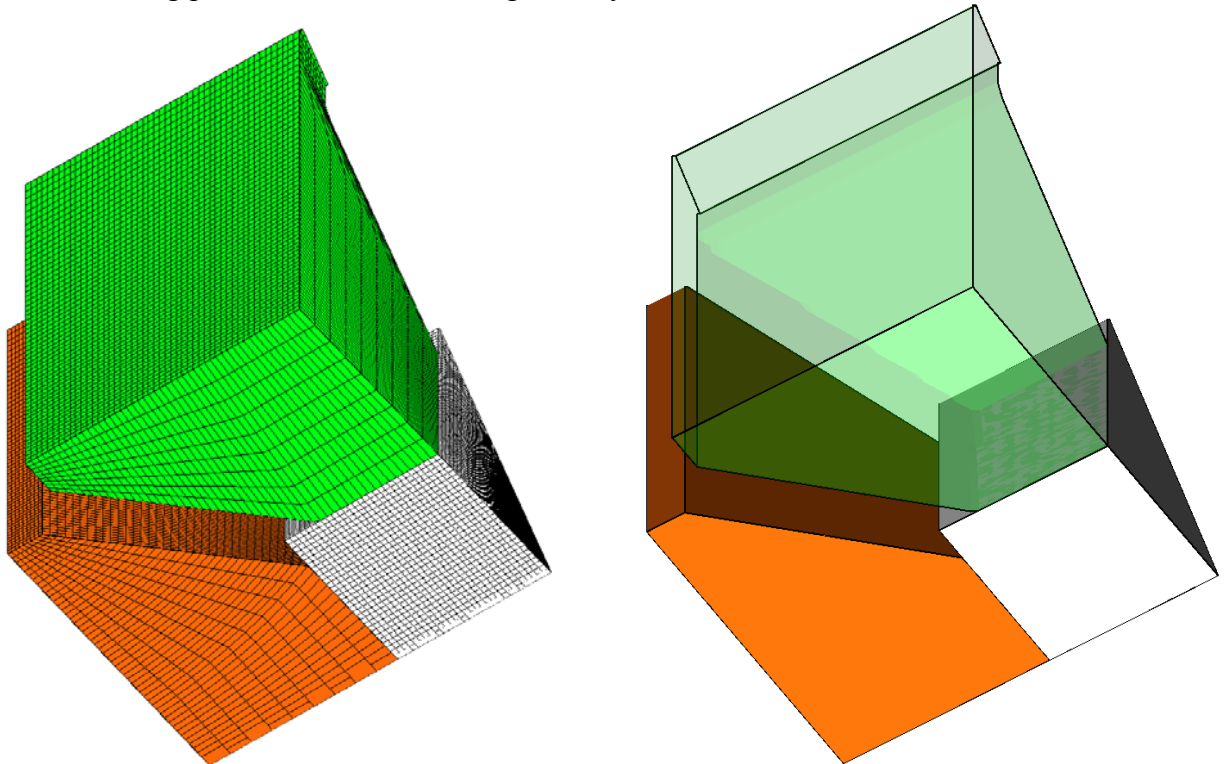


Figure 7. The initial geometry for calculation in cylindrical coordinates:

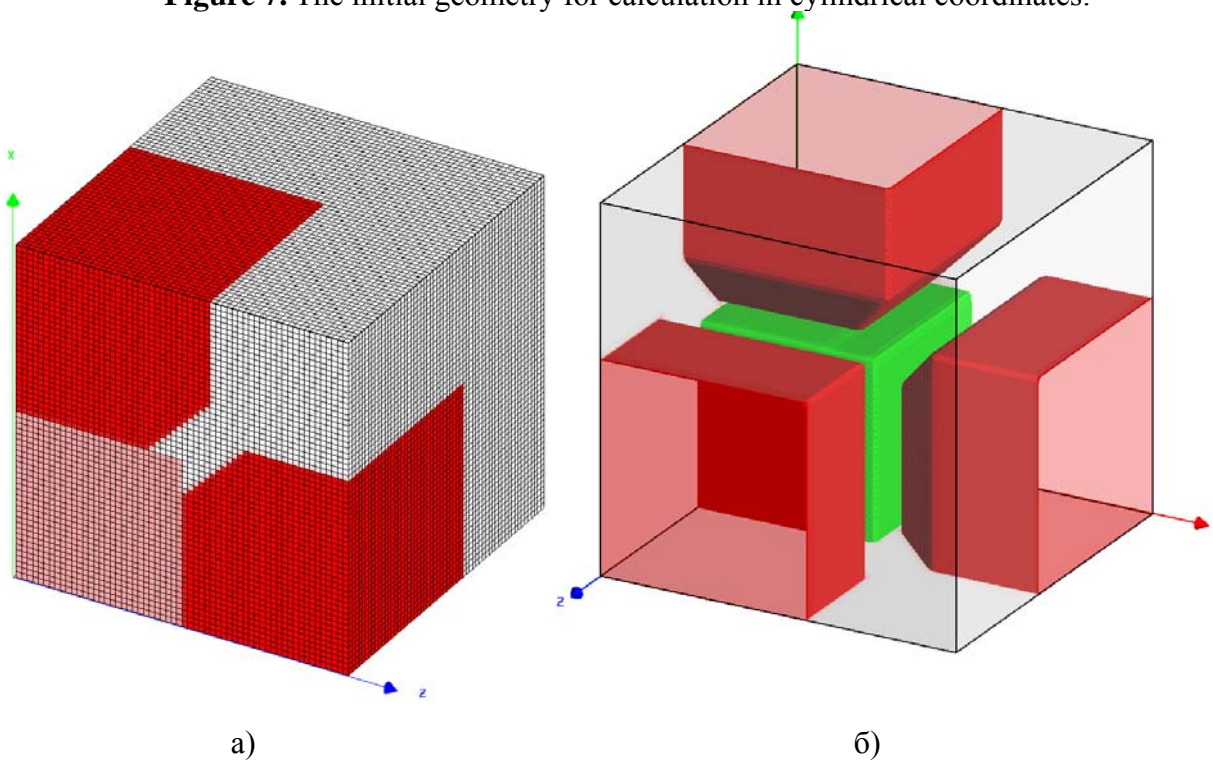


Figure 8. The initial geometry for calculation in Cartesian coordinates by the method of concentrations. Picture a) depicts different materials in different colour: red for press, pink for aluminum cube, white for air. In picture b) equiscalar surfaces show material interfaces.

The 2D and 3D calculations have been held in hydrodynamic approximation considering elastic-plastic properties in cylindrical coordinates on mixed Euler-Lagrange mesh. Press velocities vary from 1000 to 0.5 mps for 2D calculations; for 3D calculations – 100 and 10 mps. The following table represents the comparison of the results. We do not have experimental data at our disposal. Aluminum displaced mass fraction (in %) on press displacement 2.5 mm.

Calculation type	10 mps	100 mps
2D hydrodynamics +elastic-plastics	22.6	19.7
3D hydrodynamics, multiple material	29.4	27.5
3D hydrodynamics + elastic-plastics, multiple material	28.3	25.6
3D hydrodynamics in cylindrical coordinates		28.6%

The table shows that there is 1.1% difference between calculations in Cartesian coordinates by the concentrations technique and in cylindrical coordinates on Lagrangian-Euler mesh. After 10 times decreasing press velocity the aluminum displaced mass fraction increases by 2-3%. The following pictures show the shape of the detail obtained.

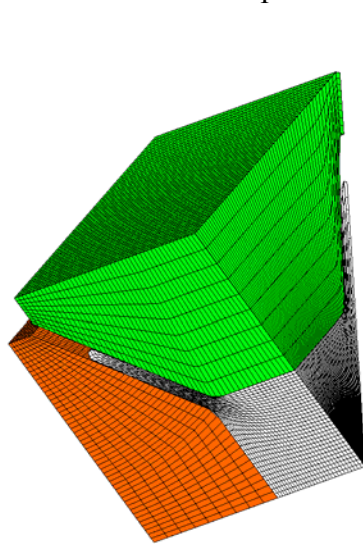


Figure 9. System state under multi-domain statement for the time of 30 μ s

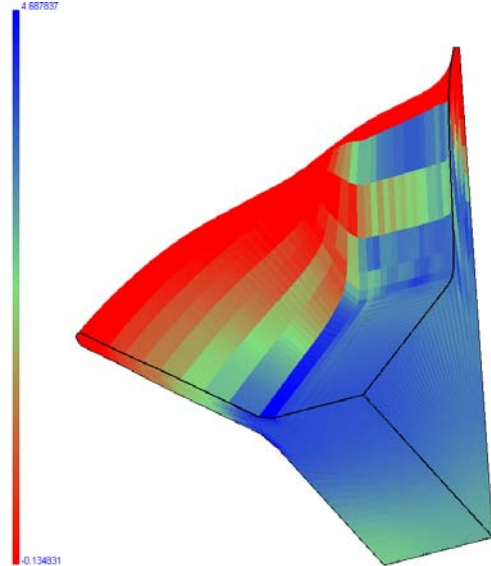


Figure 10. Pressure distribution in aluminum for the time of 30 μ s

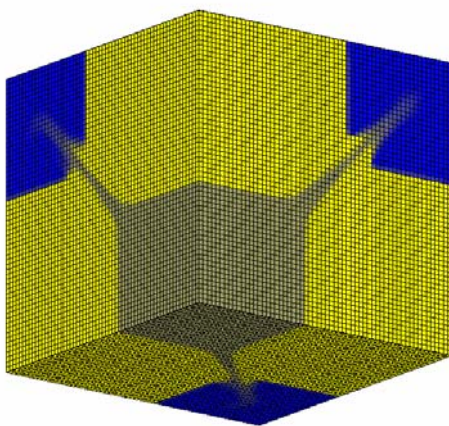


Figure11. Isometric depiction of the system for the time of 30 μ s; colouring by density.

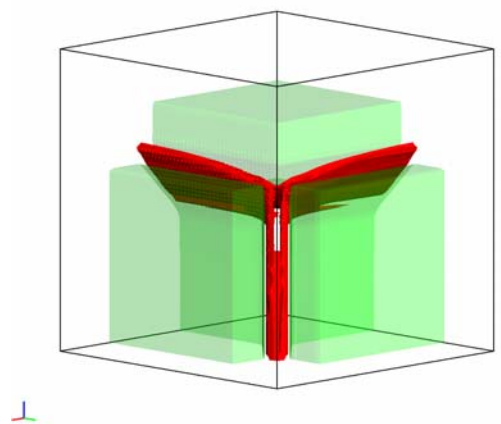


Figure 12. Temperature equiscalar surface $T=680^{\circ}\text{K}$ for the time of 30 μ s; strain 13.5%

Plane wave initiation of detonation

Three experiments were considered in which detonation in 20 mm TATB specimen was initiated by the plane shock wave [3]. The scheme of these experiments is represented in Fig 13.

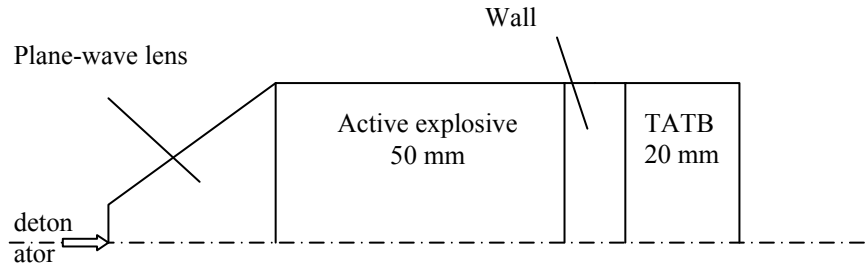


Figure 13. The scheme of the plane wave initiation of detonation. Experimental assembly diameter is 60 mm

The total time of wave passing the metal obstacle and TATB layer was measured. Then it was decreased by the calculated time of shock wave passing the obstacle to obtain the time of wave passing the TATB layer. The following table gives the comparison of simulation results and experimental data.

Experiment	Active explosive	Obstacle	The time of wave passing the TATB layer, μs / Average velocity, km/s	
			Simulation	Experiment [3]
1	Trotyl hexogen	9 mm Al	2.62 / 7.64	2.67 / 7.49
2	Octogen	6 mm Cu	2.79 / 7.16	2.89 / 6.93
3	Trotyl hexogen	6 mmCu	3.66 / 5.47	3.75 / 5.33

The simulation results are in good agreement with the experimental data. Disagreement in the wave average velocity in TATB is about 2-3%, which is commensurable with the influence of the equations of state relations indeterminacy for the materials included into buildup and with the variation of shock wave sensitivity of explosive specimens from the same lot. The truncation error in the calculation with the smeared shock wave front may be of the same order – the length of the numerical mesh cell makes 2% of the TATB layer thickness.

Shaped charge detonation

For testing code suitability to treat large deformations, there were used experimental data on shaped charges represented at VII Zababakhin Scientific Lectures, 2003.

The length of the shaped charge is 40 mm, the diameter is 32mm; initial explosive density is g/cm^3 , detonation velocity $D=8 \text{ km/s}$. Copper segment-shaped casing is 1 mil thick. The charge is point-detonated at the axis. For $Y_0=0.36\text{GPa}$, $\alpha=1$, $Y_{\text{max}}=0.4\text{GPa}$ there is a good agreement with the experiment. So at the termination time after the beginning of detonation $t=18.4 \mu\text{s}$ maximal jet diameter is 6.7 / 7.2 mm and jet length is 55 / 54 mm for calculation and experiment, respectively. **Figure 14.** shows density distribution at the sequential times.

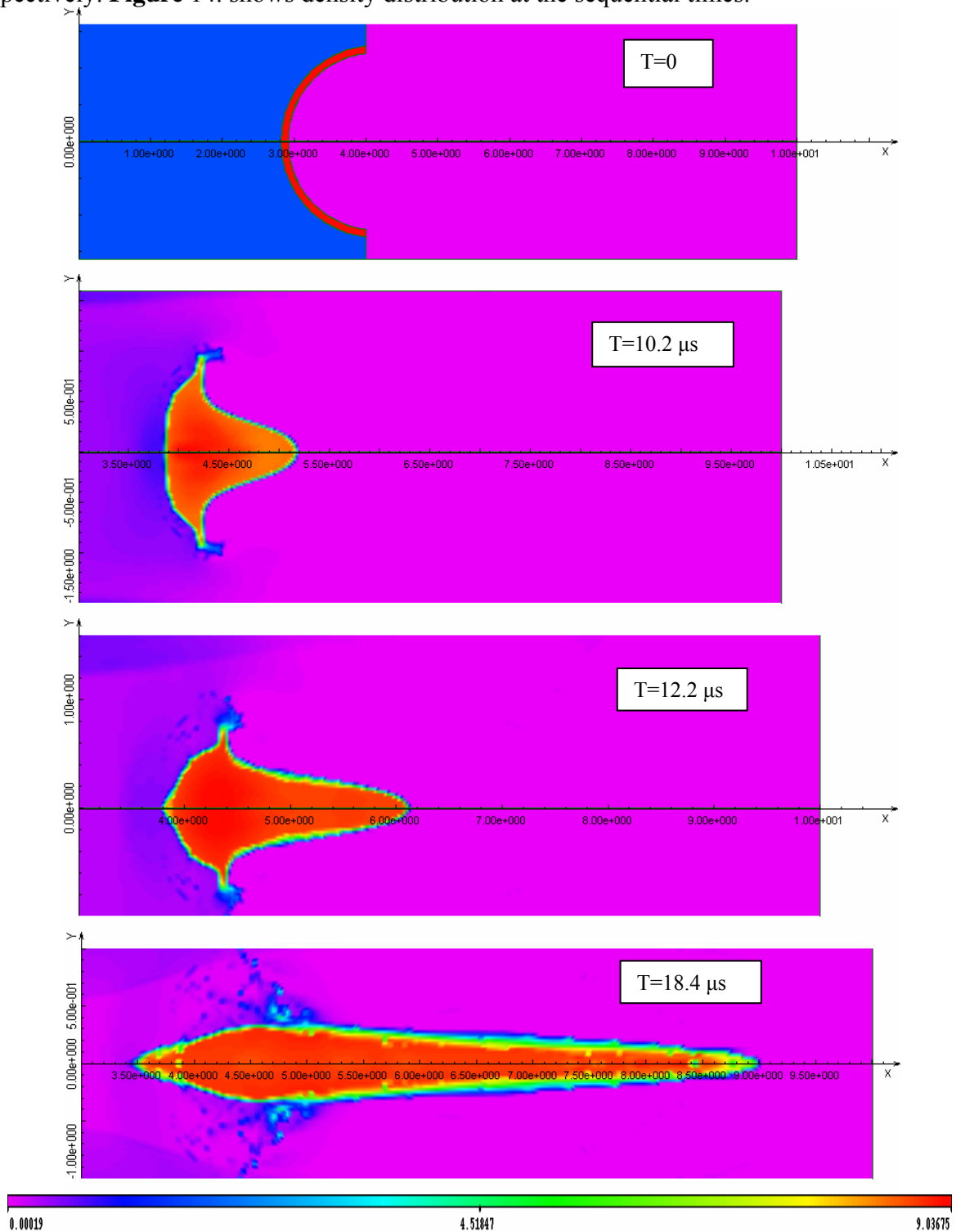


Figure 14. Density distribution

Gas transport in pipelines

In 1999-2000 GRAD-MG technique was applied to simulating the nonstationary flow of natural gas in multiple trunk-pipelines. Line section simulation module is used in the piped gas flow computer model, developed in RFNC-VNIITF /7/.

The simulation of gas flow in line section

The sea section of gas pipeline Russia-Turkey is regarded: pipe length is 386.3 km, diameter is 457 mm, the coefficient of resistance $\lambda=0.00918$, heat transfer coefficient $\alpha=7$, water temperature $T_e=8.9^\circ\text{C}$. Input gas pressure is 25 MPa, temperature 37.8°C . Output pressure is 5.40 MPa.

Initial conditions: linear boundary value distribution.

Pipeline depth varies from 0 to 2200m.

The following pictures shows flow parameters distribution on pipeline length:

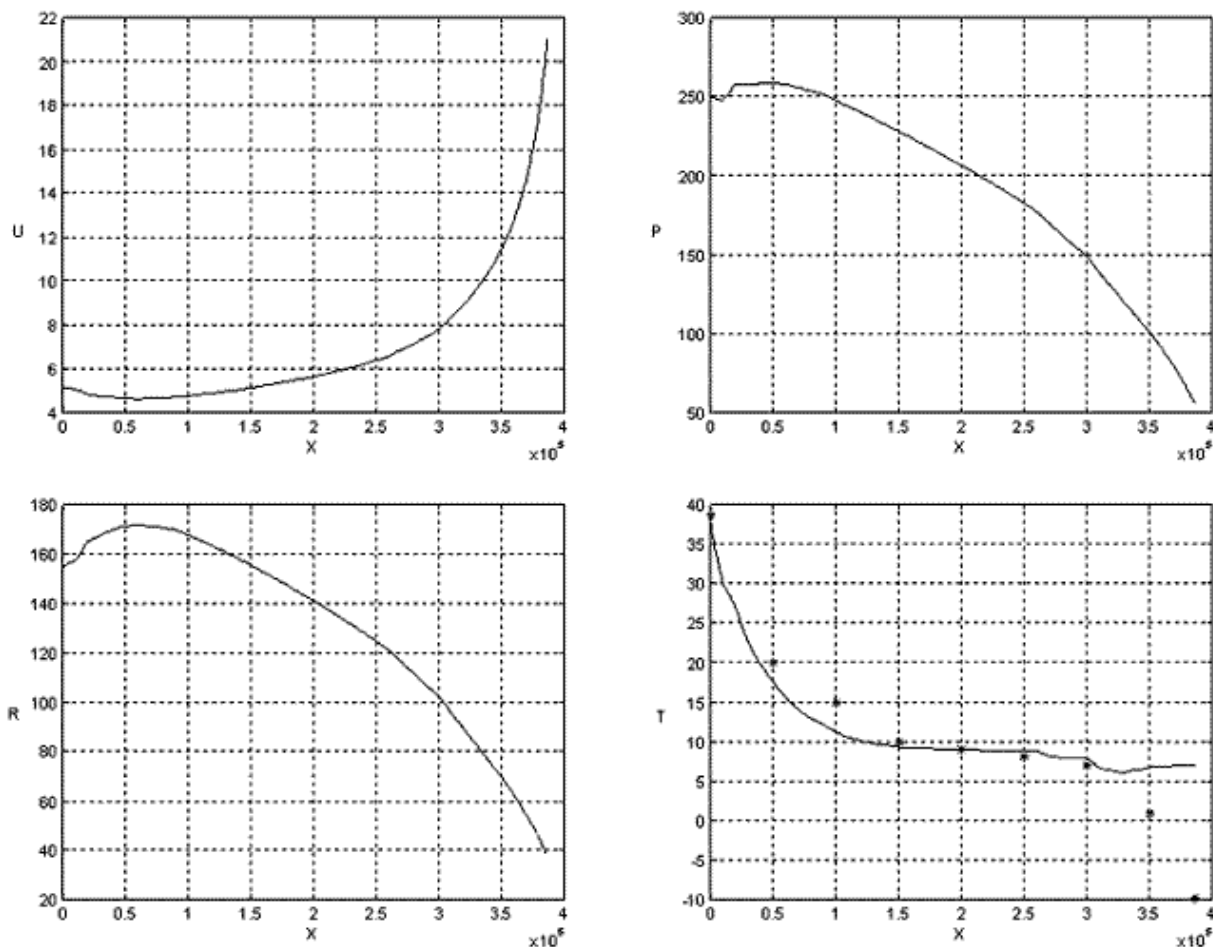


Figure 15.

Simulation of gas flow in multiple pipelines

Here is regarded the section of trunk gas-pipeline near the compressor plant KS-18 “Myshkino – Union border”, which is shown in fig.16. There are four pipes 75 km long; the fifth is 37 km long. Boom drift diameter of the third pipe is 1.4 m, others have 1.2 m. Rugosity is 0.03 mm ($\lambda=0.00918$). Soil temperature $T_e=5^\circ\text{C}$. Heat-transfer coefficients are chosen so that pipe exits have temperature indicated in figure 16.

Cross connections diameter is 1.2 m, length - 50 m. The bend (cross connection №9) is 14.7 km long; pressure is 2.0 MPa. All taps except 12 and 16 are closed. Line taps are open. Gas density at normal conditions $\rho_0=0.729277 \text{ kg/sm}^3$. The following table shows the comparison of flows calculated and measured, the difference makes $\pm 5\%$.

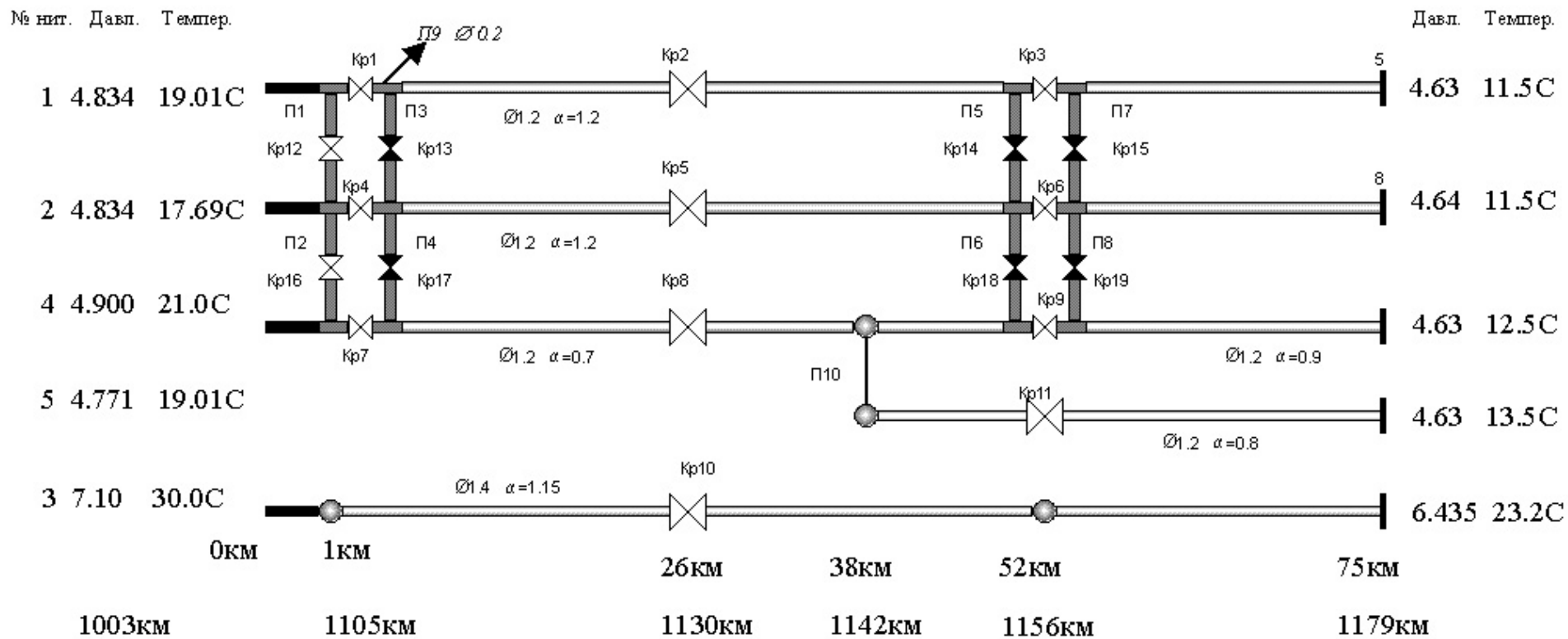


Figure 16. The scheme of the modeled section (gas flows from left to right).

4days-averaged gas flow.

№ Branch	1	2	3	4	5	Bend П9
Q SCADA	0.841	0.784	2.82	1.17		
Q calculation	0.875	0.826	2.79	1.11	0.555	0.07

References

1. Suchkov, V.A. and Shnitko, A.S., “Technique and set of program GRAD for solution of nonstationary problems of continua mechanics”, Proceedings of the Third Joint Conference on Computational Mathematics, Los Alamos, NM, USA, 23-27 January 1995 (1995).
2. Bychenkov, V.A. et al, “A method of simulating flow in compressed cubic samples”, RFNC-VNIITF Report under ISTC Project 2040 (2003).
3. Aminov, Y.A., Vershinin, A.V., Eskov, N.S. et al, “Research on shock sensitivity of a TATB-based plastic explosive”, *Combustion and Explosion Physics*, **1**, 103-108, 1995 (1995).
4. Grebyonkin, K.F., “A semiconductor model of TATB detonation”, Proceedings of the V Zababakhin Talks Conference, Snezhinsk, 21-25 September 1998 (1999).
5. Tonks, D.L., “The data shop: A database of weak-shock constitutive data”, LANL Report LA-12068-MS (1991).
6. Glushak, A.B. and Novikov, S.A., “High-rate plastic straining of metals”, *Chemical Physics*, V.19, 2, 65-69 (2000)
7. Anuchin, M.G., Gagarin, S.V., Ignatiev, A.O., Kalinin, A.A., Kuznetsov, A.N., Suchkov, V.A., and Shnitko, A.S., “A nonstationary model of piped gas flow”, Book of Abstracts, DISCOM 2002 Conference, Moscow, November 2002 (2002).